

Supplementary Material

Bayesian Structural Inference for Hidden Processes

Christopher C. Strelieff and James P. Crutchfield

I. OVERVIEW

The supplementary materials provide tables and figures that lend an in-depth picture of the Bayesian Structural Inference examples. Unless otherwise noted, all analyses presented here use the same single data series and parameter settings detailed in the main text. Please use the main text as the primary guide.

The first three sections address the Golden Mean, Even, and SNS processes. Each provides a table of estimates of h_μ and C_μ using the complete set \mathcal{M} of one- to five-state ϵ -machines denoted. Estimates are given for each subsample length $L = 2^i$, where $i = 0, 1, 2, \dots, 17$, as in the main text. To be clear, this means that we analyze subsamples $D_{0:L} = x_0x_1x_2\dots x_{L-1}$ using different initial segments of a single long data series, allowing for a consistent view of estimate convergence. For both information-theoretic quantities, we list the posterior mean and equal-tailed, 95% credible interval (CI) constructed using the 2.5% and 97.5% quantiles estimated from 50,000 samples of the posterior distribution. The CI is denoted by parenthesized number pairs. A second table provides the same estimates of h_μ and C_μ using only the M_{MAP} model. As a result, this table no longer reflects uncertainty in model topology, which may be small or large depending on the data and subsample length under consideration. An additional column in this second table provides the MAP topology along with its posterior probability. The latter is denoted in parentheses.

In addition to the tables of estimates, figures demonstrate the convergence of h_μ and C_μ marginal posterior distributions as a function subsample length L . In this, we consider the difference between posteriors using the complete set \mathcal{M} of candidate models and those that only employ the MAP topology. This set of figures also illustrates the difference between $\beta = 4$ and $\beta = 2$. (We use different data, but still a single time series, for the $\beta = 2$ example.) In all plots the marginal posterior distribution for the quantity of interest is estimated using a Gaussian kernel density estimation (Gkde) of the density using 50,000 samples from the appropriate density. If there is little or no variation in the samples the Gkde fails and no density is drawn. This happens, for example, when the MAP topology has one state, and $C_\mu = 0$, for small data sizes. Posterior samples are valid, however, and posterior mean and credible interval can be provided (see tables).

Section V plots the number of accepting topologies as a function of subsample length for each of the example data sources in Fig. S10. The panels demonstrate that there are many valid candidate topologies for a given data series, even when subsamples of considerable length are available.

Finally, Sec. VI illustrates all topologies that met the MAP criterion for the data sources considered. Notably, there are not many structures to consider despite the large number of topologies that accept the data.

II. GOLDEN MEAN PROCESS: STRUCTURAL INFERENCE

TABLE S1. Inference of Golden Mean Process properties using \mathcal{M} , $\beta = 4$.

L	h_μ	C_μ
1	6.767e-01 (3.682e-02, 9.994e-01)	1.467e-01 (0.000e+00, 1.333e+00)
2	6.400e-01 (6.662e-02, 9.990e-01)	1.074e-01 (0.000e+00, 1.089e+00)
4	7.771e-01 (2.760e-01, 9.996e-01)	1.146e-01 (0.000e+00, 1.000e+00)
8	7.753e-01 (3.557e-01, 9.994e-01)	1.441e-01 (0.000e+00, 1.000e+00)
16	7.941e-01 (4.751e-01, 9.976e-01)	1.128e-01 (0.000e+00, 9.469e-01)
32	7.697e-01 (5.221e-01, 9.773e-01)	2.564e-01 (0.000e+00, 1.556e+00)
64	6.440e-01 (5.207e-01, 6.942e-01)	1.052e+00 (8.235e-01, 1.797e+00)
128	6.575e-01 (5.953e-01, 6.930e-01)	9.209e-01 (8.667e-01, 9.590e-01)
256	6.684e-01 (6.311e-01, 6.917e-01)	9.128e-01 (8.740e-01, 9.437e-01)
512	6.718e-01 (6.477e-01, 6.889e-01)	9.107e-01 (8.835e-01, 9.338e-01)
1024	6.622e-01 (6.428e-01, 6.780e-01)	9.217e-01 (9.048e-01, 9.369e-01)
2048	6.618e-01 (6.483e-01, 6.736e-01)	9.225e-01 (9.107e-01, 9.333e-01)
4096	6.587e-01 (6.490e-01, 6.678e-01)	9.253e-01 (9.172e-01, 9.329e-01)
8192	6.645e-01 (6.582e-01, 6.704e-01)	9.203e-01 (9.143e-01, 9.259e-01)
16384	6.643e-01 (6.599e-01, 6.685e-01)	9.205e-01 (9.164e-01, 9.245e-01)
32768	6.647e-01 (6.615e-01, 6.676e-01)	9.202e-01 (9.173e-01, 9.231e-01)
65536	6.662e-01 (6.640e-01, 6.682e-01)	9.188e-01 (9.167e-01, 9.208e-01)
131072	6.670e-01 (6.655e-01, 6.684e-01)	9.180e-01 (9.165e-01, 9.194e-01)

TABLE S2. Inference of Golden Mean Process properties using M_{MAP} , $\beta = 4$.

L	h_μ	C_μ	MAP Topology
1	7.221e-01 (9.729e-02, 9.996e-01)	0.000e+00 (0.000e+00, 0.000e+00)	n1k2id3 (8.570e-01)
2	6.603e-01 (6.849e-02, 9.992e-01)	0.000e+00 (0.000e+00, 0.000e+00)	n1k2id3 (8.954e-01)
4	8.116e-01 (3.066e-01, 9.997e-01)	0.000e+00 (0.000e+00, 0.000e+00)	n1k2id3 (8.896e-01)
8	8.129e-01 (3.811e-01, 9.995e-01)	0.000e+00 (0.000e+00, 0.000e+00)	n1k2id3 (8.600e-01)
16	8.141e-01 (4.787e-01, 9.981e-01)	0.000e+00 (0.000e+00, 0.000e+00)	n1k2id3 (8.795e-01)
32	8.134e-01 (5.668e-01, 9.830e-01)	0.000e+00 (0.000e+00, 0.000e+00)	n1k2id3 (7.324e-01)
64	6.636e-01 (5.842e-01, 6.942e-01)	9.061e-01 (8.188e-01, 9.622e-01)	n2k2id5 (7.873e-01)
128	6.577e-01 (5.962e-01, 6.929e-01)	9.198e-01 (8.666e-01, 9.583e-01)	n2k2id5 (9.971e-01)
256	6.684e-01 (6.316e-01, 6.918e-01)	9.125e-01 (8.736e-01, 9.433e-01)	n2k2id5 (9.987e-01)
512	6.717e-01 (6.477e-01, 6.889e-01)	9.108e-01 (8.836e-01, 9.338e-01)	n2k2id5 (9.994e-01)
1024	6.621e-01 (6.429e-01, 6.781e-01)	9.217e-01 (9.046e-01, 9.369e-01)	n2k2id5 (9.997e-01)
2048	6.617e-01 (6.481e-01, 6.735e-01)	9.226e-01 (9.108e-01, 9.335e-01)	n2k2id5 (9.998e-01)
4096	6.588e-01 (6.491e-01, 6.677e-01)	9.253e-01 (9.172e-01, 9.328e-01)	n2k2id5 (9.999e-01)
8192	6.645e-01 (6.582e-01, 6.705e-01)	9.202e-01 (9.143e-01, 9.259e-01)	n2k2id5 (1.000e+00)
16384	6.643e-01 (6.599e-01, 6.685e-01)	9.205e-01 (9.164e-01, 9.245e-01)	n2k2id5 (1.000e+00)
32768	6.646e-01 (6.616e-01, 6.677e-01)	9.202e-01 (9.173e-01, 9.231e-01)	n2k2id5 (1.000e+00)
65536	6.662e-01 (6.640e-01, 6.682e-01)	9.188e-01 (9.167e-01, 9.208e-01)	n2k2id5 (1.000e+00)
131072	6.670e-01 (6.655e-01, 6.684e-01)	9.180e-01 (9.165e-01, 9.194e-01)	n2k2id5 (1.000e+00)

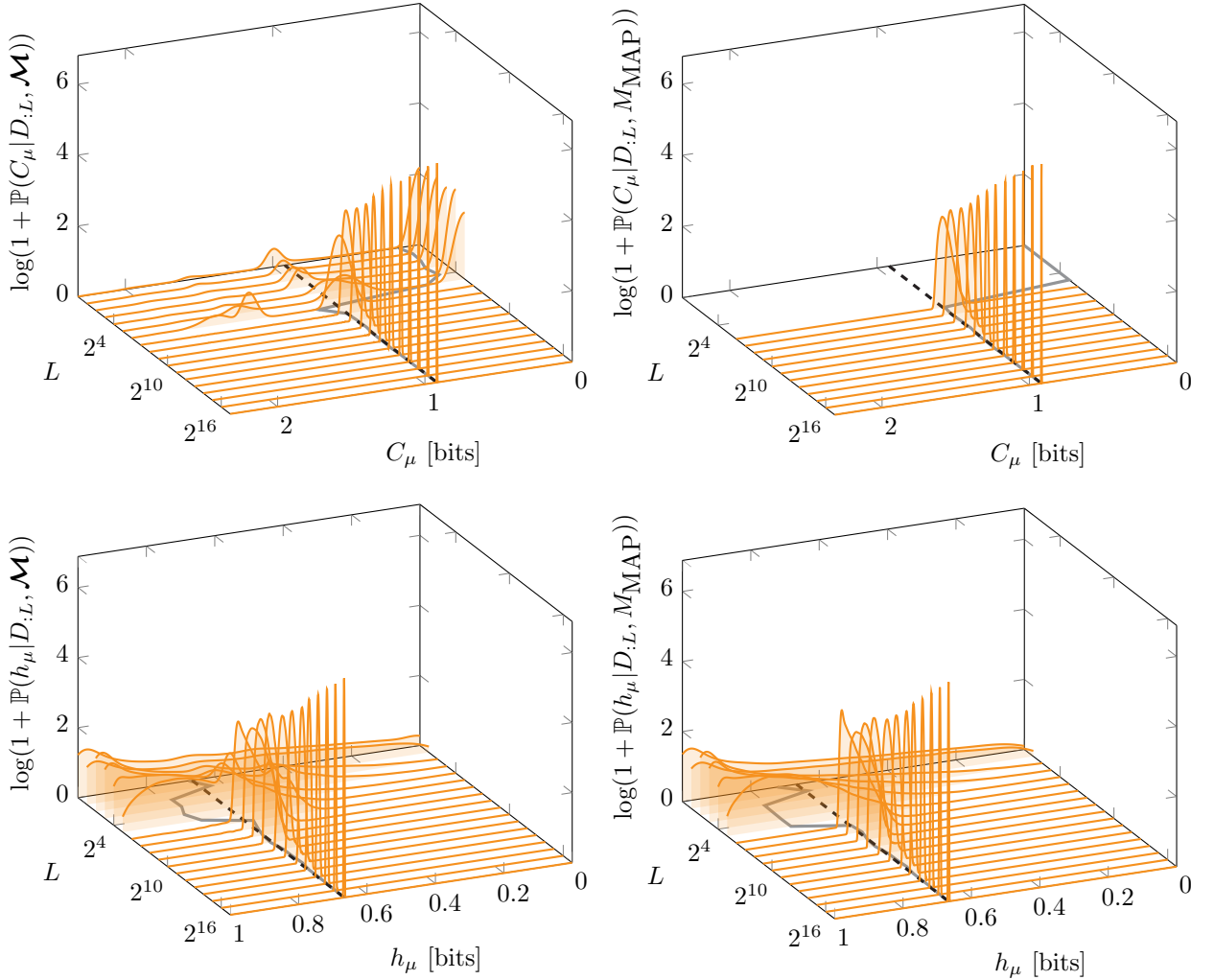


FIG. S1. Golden Mean Process, $\beta = 4$: Convergence of the posterior densities for C_μ (top) and h_μ (bottom) as a function of subsample length L using the set of all topological ϵ -machines with 1-5 states \mathcal{M} (left column) and the maximum a posteriori model M_{MAP} (right column). In each panel, the black, dashed line indicates the true value and the gray, solid line shows the posterior mean.

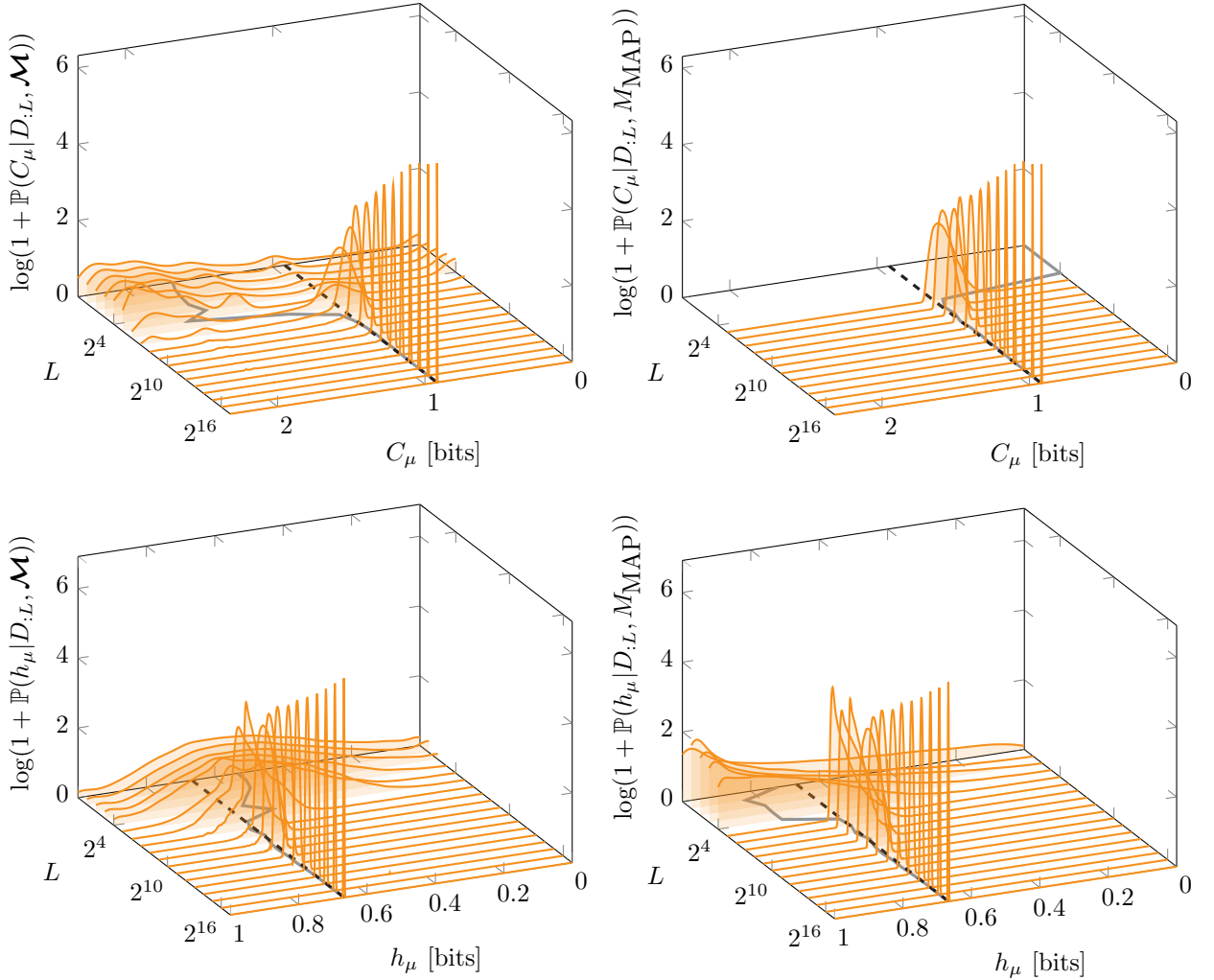


FIG. S2. Golden Mean Process, $\beta = 2$: Convergence of the posterior densities for C_μ (top) and h_μ (bottom) as a function of subsample length L using the set of all topological ϵ -machines with 1-5 states \mathcal{M} (left column) and the maximum a posteriori model M_{MAP} (right column). In each panel, the black, dashed line indicates the true value and the gray, solid line shows the posterior mean. Contrast these panels with those in Figure S1, where the penalty for structure is higher.

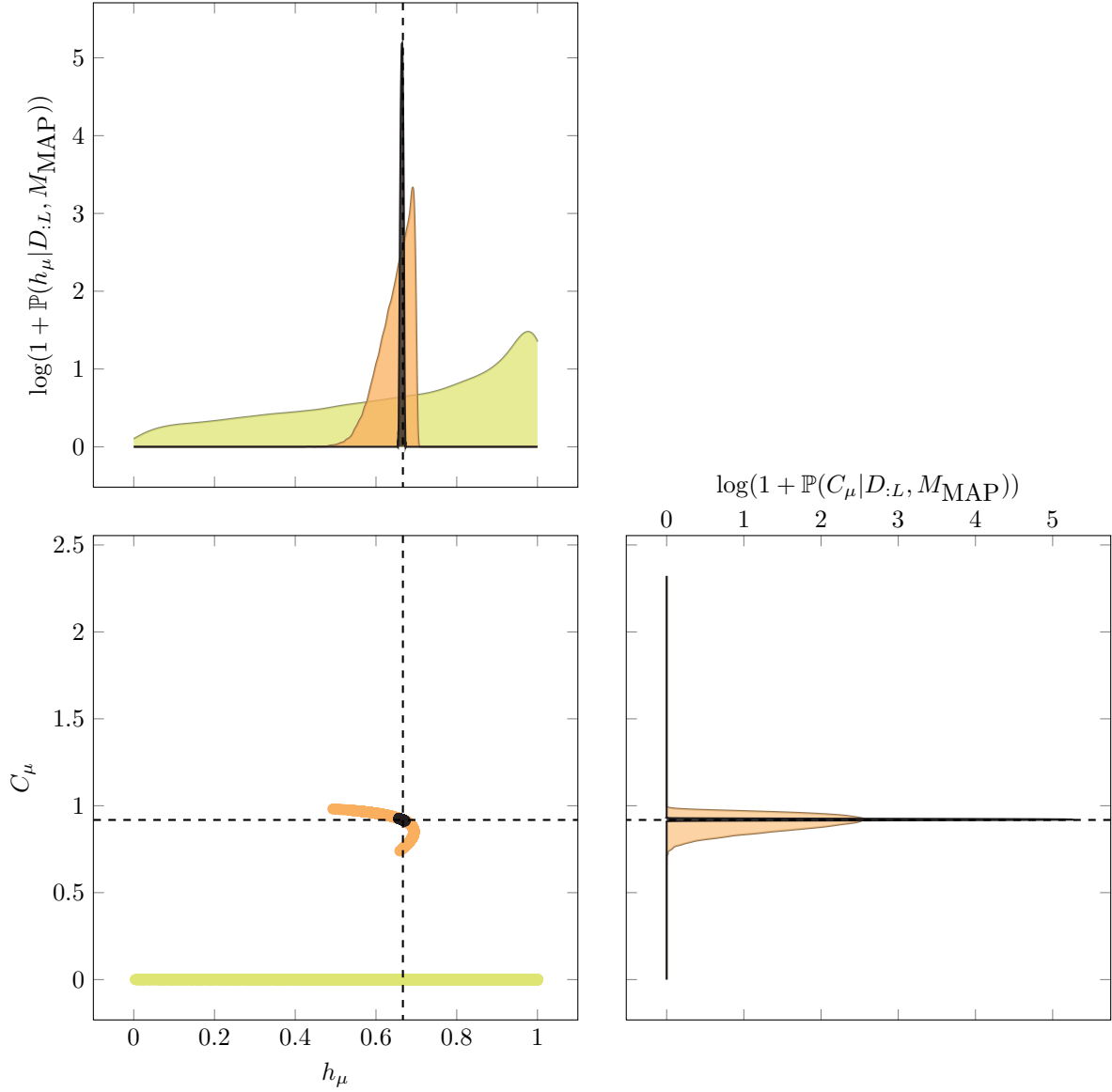


FIG. S3. Golden Mean Process, $\beta = 4$: Joint distribution samples using the MAP model at the given lengths instead of the full set of candidate models. Colors correspond to data subsample length, as in previous plots. The MAP topology for $L = 1$ (light/beige) has one state and $C_\mu = 0$, as indicated by the samples in the $h_\mu - C_\mu$ plane. No Gkde approximation of these samples is provided due to this complete lack of variation.

III. EVEN PROCESS: STRUCTURAL INFERENCE

TABLE S3. Inference of Even Process properties using \mathcal{M} , $\beta = 4$.

L	h_μ	C_μ
1	6.777e-01 (3.811e-02, 9.994e-01)	1.480e-01 (0.000e+00, 1.388e+00)
2	7.414e-01 (0.000e+00, 9.997e-01)	2.222e-01 (0.000e+00, 1.528e+00)
4	7.697e-01 (2.359e-01, 9.996e-01)	1.191e-01 (0.000e+00, 1.224e+00)
8	8.572e-01 (4.097e-01, 9.998e-01)	1.249e-01 (0.000e+00, 1.422e+00)
16	8.235e-01 (4.751e-01, 9.998e-01)	3.080e-01 (0.000e+00, 9.454e-01)
32	6.457e-01 (4.655e-01, 9.616e-01)	6.909e-01 (0.000e+00, 8.961e-01)
64	6.804e-01 (6.276e-01, 6.942e-01)	8.746e-01 (7.675e-01, 9.464e-01)
128	6.824e-01 (6.453e-01, 6.942e-01)	8.854e-01 (8.166e-01, 9.359e-01)
256	6.783e-01 (6.485e-01, 6.939e-01)	8.993e-01 (8.568e-01, 9.333e-01)
512	6.679e-01 (6.422e-01, 6.868e-01)	9.151e-01 (8.890e-01, 9.374e-01)
1024	6.756e-01 (6.602e-01, 6.874e-01)	9.069e-01 (8.875e-01, 9.243e-01)
2048	6.700e-01 (6.581e-01, 6.801e-01)	9.144e-01 (9.016e-01, 9.260e-01)
4096	6.666e-01 (6.578e-01, 6.744e-01)	9.181e-01 (9.096e-01, 9.263e-01)
8192	6.704e-01 (6.647e-01, 6.757e-01)	9.142e-01 (9.080e-01, 9.202e-01)
16384	6.666e-01 (6.623e-01, 6.707e-01)	9.183e-01 (9.141e-01, 9.225e-01)
32768	6.660e-01 (6.629e-01, 6.689e-01)	9.189e-01 (9.160e-01, 9.219e-01)
65536	6.657e-01 (6.635e-01, 6.677e-01)	9.193e-01 (9.172e-01, 9.213e-01)
131072	6.658e-01 (6.643e-01, 6.672e-01)	9.192e-01 (9.177e-01, 9.206e-01)

TABLE S4. Inference of Even Process properties using M_{MAP} , $\beta = 4$.

L	h_μ	C_μ	MAP Topology
1	7.226e-01 (1.003e-01, 9.996e-01)	0.000e+00 (0.000e+00, 0.000e+00)	n1k2id3 (8.570e-01)
2	8.426e-01 (3.541e-01, 9.998e-01)	0.000e+00 (0.000e+00, 0.000e+00)	n1k2id3 (7.893e-01)
4	8.100e-01 (2.982e-01, 9.997e-01)	0.000e+00 (0.000e+00, 0.000e+00)	n1k2id3 (8.721e-01)
8	9.027e-01 (5.764e-01, 9.999e-01)	0.000e+00 (0.000e+00, 0.000e+00)	n1k2id3 (8.626e-01)
16	9.517e-01 (7.735e-01, 9.999e-01)	0.000e+00 (0.000e+00, 0.000e+00)	n1k2id3 (6.023e-01)
32	6.316e-01 (4.650e-01, 6.941e-01)	7.152e-01 (4.825e-01, 8.861e-01)	n2k2id7 (9.434e-01)
64	6.802e-01 (6.282e-01, 6.942e-01)	8.728e-01 (7.690e-01, 9.445e-01)	n2k2id7 (9.941e-01)
128	6.823e-01 (6.456e-01, 6.942e-01)	8.845e-01 (8.165e-01, 9.351e-01)	n2k2id7 (9.973e-01)
256	6.783e-01 (6.483e-01, 6.939e-01)	8.991e-01 (8.566e-01, 9.334e-01)	n2k2id7 (9.989e-01)
512	6.681e-01 (6.426e-01, 6.869e-01)	9.149e-01 (8.887e-01, 9.370e-01)	n2k2id7 (9.995e-01)
1024	6.757e-01 (6.604e-01, 6.873e-01)	9.068e-01 (8.878e-01, 9.241e-01)	n2k2id7 (9.997e-01)
2048	6.700e-01 (6.581e-01, 6.801e-01)	9.143e-01 (9.017e-01, 9.260e-01)	n2k2id7 (9.999e-01)
4096	6.666e-01 (6.579e-01, 6.744e-01)	9.181e-01 (9.096e-01, 9.262e-01)	n2k2id7 (9.999e-01)
8192	6.704e-01 (6.647e-01, 6.757e-01)	9.142e-01 (9.080e-01, 9.202e-01)	n2k2id7 (1.000e+00)
16384	6.666e-01 (6.623e-01, 6.707e-01)	9.183e-01 (9.141e-01, 9.224e-01)	n2k2id7 (1.000e+00)
32768	6.660e-01 (6.629e-01, 6.689e-01)	9.189e-01 (9.160e-01, 9.219e-01)	n2k2id7 (1.000e+00)
65536	6.657e-01 (6.635e-01, 6.678e-01)	9.193e-01 (9.172e-01, 9.213e-01)	n2k2id7 (1.000e+00)
131072	6.658e-01 (6.642e-01, 6.672e-01)	9.192e-01 (9.177e-01, 9.207e-01)	n2k2id7 (1.000e+00)

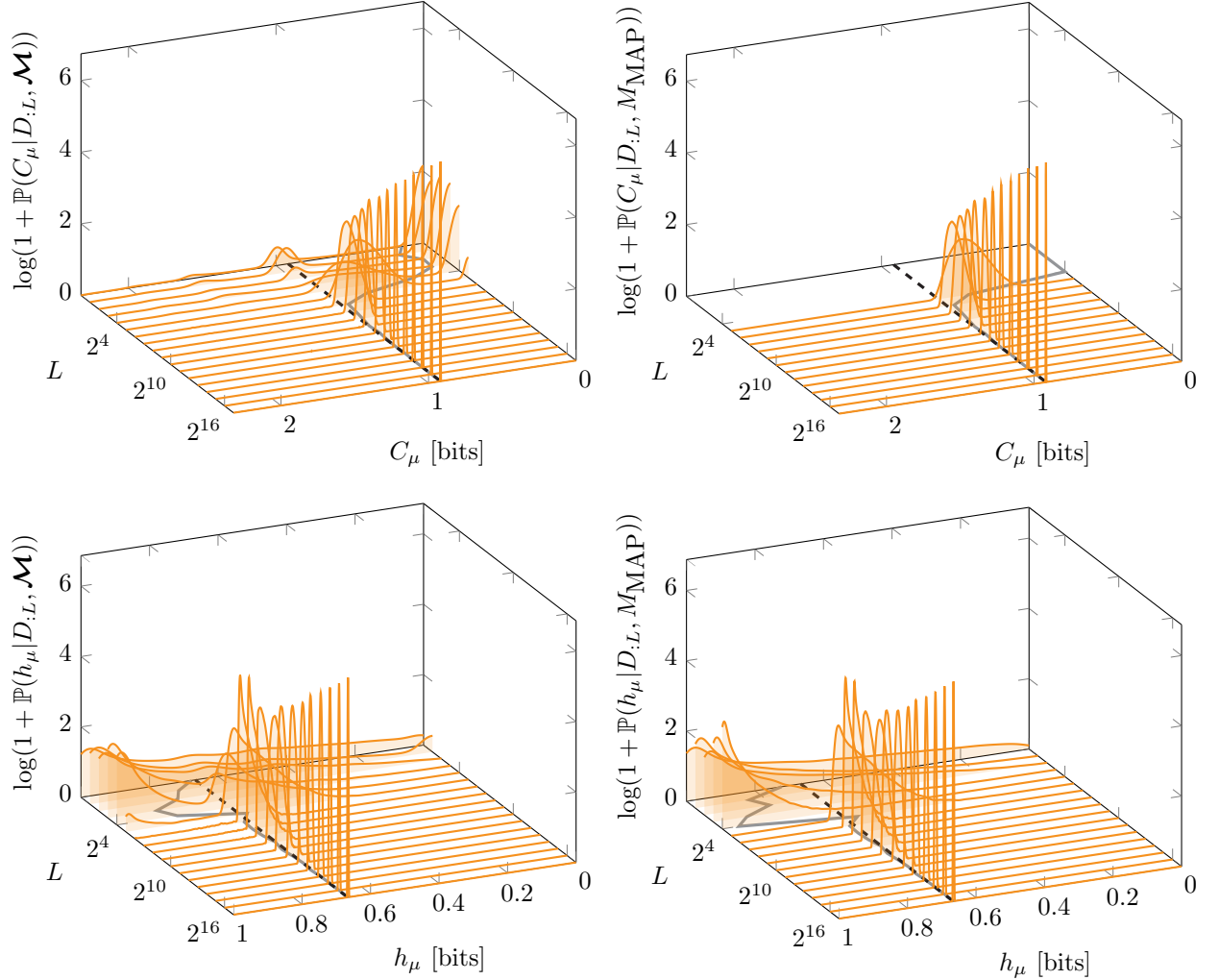


FIG. S4. Even Process, $\beta = 4$: Convergence of the posterior densities for C_μ (top) and h_μ (bottom) as a function of subsample length L using the set of all topological ϵ -machines with one- to five-states \mathcal{M} (left column) and the maximum a posteriori model M_{MAP} (right column). In each panel, the black, dashed line indicates the true value and the gray, solid line shows the posterior mean.

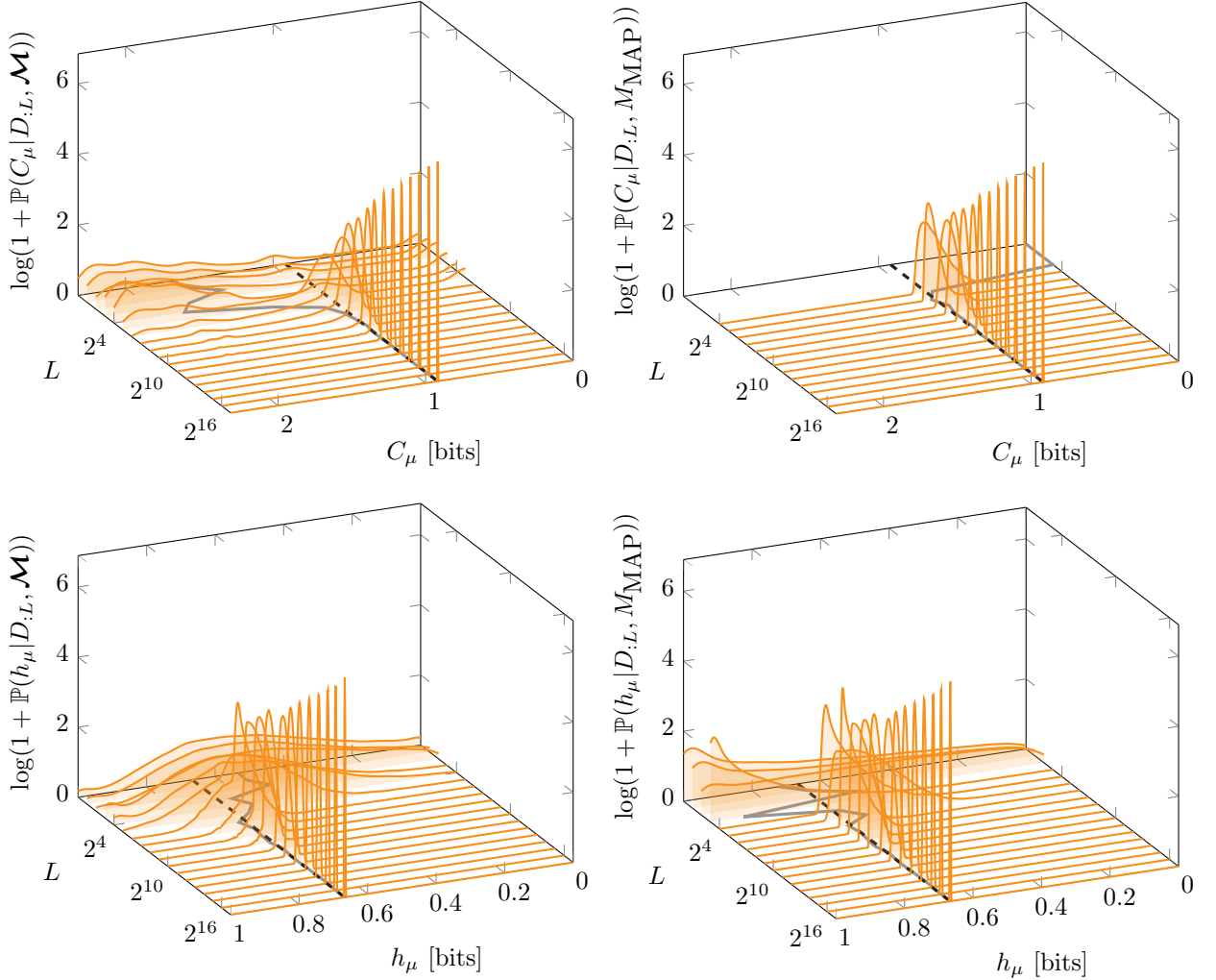


FIG. S5. Even Process, $\beta = 2$: Convergence of the posterior densities for C_μ (top) and h_μ (bottom) as a function of subsample length L using the set of all topological ϵ -machines with one- to five-states \mathcal{M} (left column) and the maximum a posteriori model M_{MAP} (right column). In each panel, the black, dashed line indicates the true value and the gray, solid line shows the posterior mean.

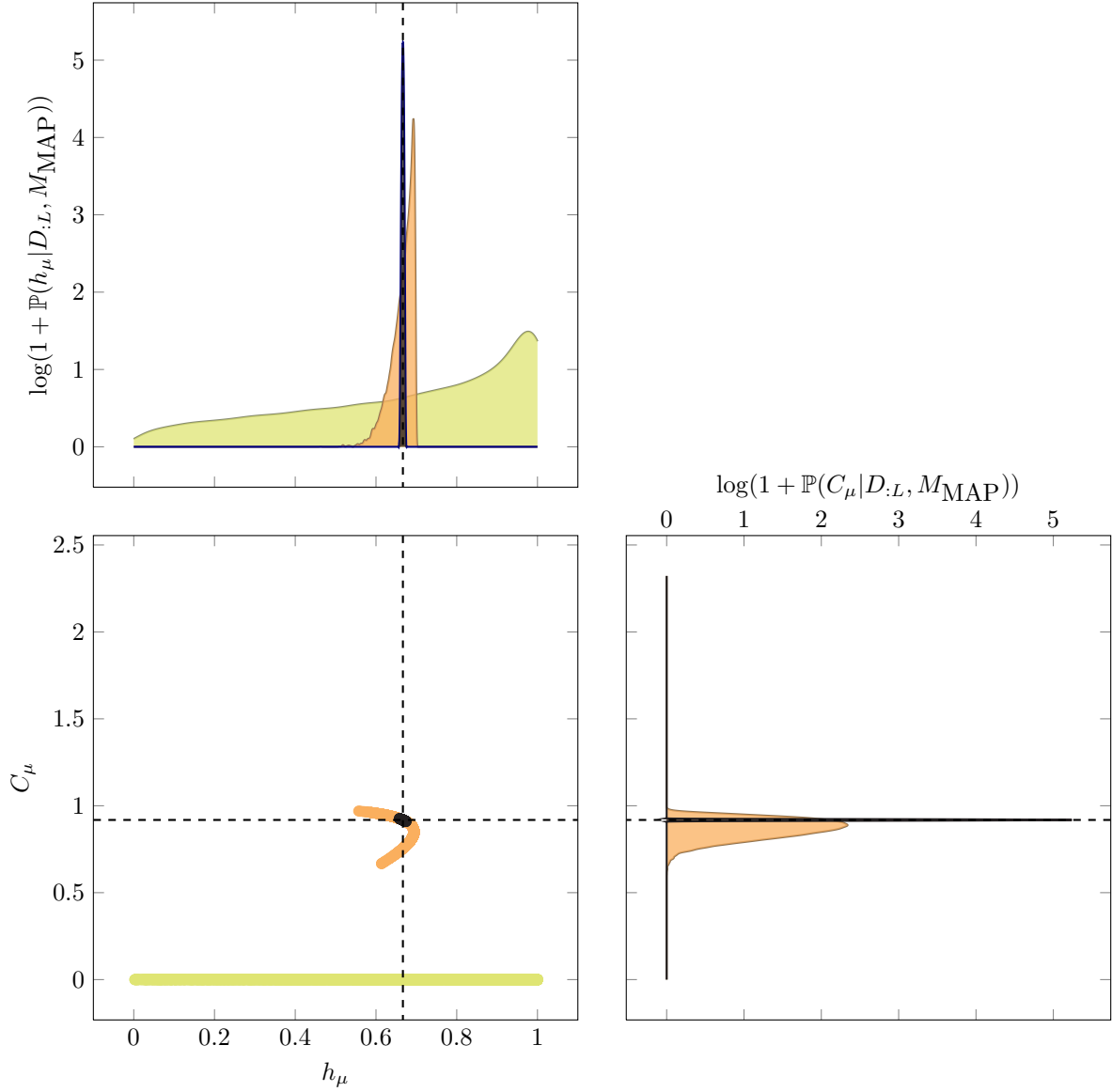


FIG. S6. Even Process, $\beta = 4$: Samples of the joint distribution using the MAP model at the given lengths instead of the full set of candidate models. Colors correspond to data subsample length, as in previous plots. The MAP topology for $L = 1$ (light/beige) has one state and $C_\mu = 0$, as indicated by the samples in the $h_\mu - C_\mu$ plane. No Gkde approximation of these samples is provided due to this complete lack of variation.

IV. SNS PROCESS: STRUCTURAL INFERENCE

TABLE S5. Inference of SNS Process properties using \mathcal{M} , $\beta = 4$.

L	h_μ	C_μ
1	6.780e-01 (3.817e-02,9.993e-01)	1.483e-01 (0.000e+00,1.325e+00)
2	7.425e-01 (0.000e+00,9.997e-01)	2.207e-01 (0.000e+00,1.525e+00)
4	7.698e-01 (2.398e-01,9.997e-01)	1.207e-01 (0.000e+00,1.225e+00)
8	7.781e-01 (3.449e-01,9.994e-01)	1.326e-01 (0.000e+00,1.357e+00)
16	7.952e-01 (2.702e-01,9.994e-01)	3.679e-01 (0.000e+00,2.084e+00)
32	7.555e-01 (4.978e-01,9.605e-01)	8.161e-02 (0.000e+00,8.579e-01)
64	7.228e-01 (5.935e-01,9.142e-01)	4.627e-01 (0.000e+00,1.043e+00)
128	6.808e-01 (6.365e-01,6.942e-01)	8.006e-01 (6.982e-01,8.808e-01)
256	6.756e-01 (6.411e-01,6.937e-01)	7.801e-01 (7.088e-01,8.407e-01)
512	6.799e-01 (6.562e-01,6.929e-01)	8.151e-01 (7.419e-01,1.390e+00)
1024	6.849e-01 (6.693e-01,6.931e-01)	9.021e-01 (7.717e-01,1.757e+00)
2048	6.827e-01 (6.701e-01,6.922e-01)	1.441e+00 (7.905e-01,2.219e+00)
4096	6.825e-01 (6.756e-01,6.896e-01)	1.787e+00 (1.673e+00,2.228e+00)
8192	6.828e-01 (6.782e-01,6.874e-01)	2.002e+00 (1.692e+00,2.233e+00)
16384	6.800e-01 (6.769e-01,6.832e-01)	2.198e+00 (2.168e+00,2.231e+00)
32768	6.789e-01 (6.766e-01,6.811e-01)	2.197e+00 (2.170e+00,2.229e+00)
65536	6.784e-01 (6.769e-01,6.800e-01)	2.199e+00 (2.174e+00,2.228e+00)
131072	6.788e-01 (6.777e-01,6.799e-01)	2.201e+00 (2.178e+00,2.230e+00)

TABLE S6. Inference of SNS Process properties using M_{MAP} , $\beta = 4$.

L	h_μ	C_μ	MAP Topology
1	7.231e-01 (9.607e-02,9.996e-01)	0.000e+00 (0.000e+00,0.000e+00)	n1k2id3 (8.570e-01)
2	8.414e-01 (3.462e-01,9.998e-01)	0.000e+00 (0.000e+00,0.000e+00)	n1k2id3 (7.893e-01)
4	8.086e-01 (2.981e-01,9.997e-01)	0.000e+00 (0.000e+00,0.000e+00)	n1k2id3 (8.721e-01)
8	8.136e-01 (3.826e-01,9.996e-01)	0.000e+00 (0.000e+00,0.000e+00)	n1k2id3 (8.829e-01)
16	8.800e-01 (5.927e-01,9.997e-01)	0.000e+00 (0.000e+00,0.000e+00)	n1k2id3 (7.774e-01)
32	7.665e-01 (5.040e-01,9.641e-01)	0.000e+00 (0.000e+00,0.000e+00)	n1k2id3 (9.105e-01)
64	6.712e-01 (5.947e-01,6.942e-01)	7.842e-01 (6.406e-01,8.918e-01)	n2k2id5 (5.301e-01)
128	6.803e-01 (6.370e-01,6.942e-01)	7.981e-01 (7.021e-01,8.756e-01)	n2k2id5 (9.835e-01)
256	6.755e-01 (6.408e-01,6.937e-01)	7.786e-01 (7.083e-01,8.393e-01)	n2k2id5 (9.953e-01)
512	6.804e-01 (6.600e-01,6.928e-01)	7.887e-01 (7.416e-01,8.313e-01)	n2k2id5 (9.721e-01)
1024	6.858e-01 (6.746e-01,6.929e-01)	8.029e-01 (7.714e-01,8.321e-01)	n2k2id5 (8.989e-01)
2048	6.871e-01 (6.801e-01,6.922e-01)	8.066e-01 (7.848e-01,8.273e-01)	n2k2id5 (3.419e-01)
4096	6.826e-01 (6.760e-01,6.893e-01)	1.703e+00 (1.672e+00,1.733e+00)	n4k2id3334 (1.336e-01)
8192	6.834e-01 (6.792e-01,6.877e-01)	1.709e+00 (1.687e+00,1.730e+00)	n4k2id3334 (6.462e-02)
16384	6.800e-01 (6.769e-01,6.831e-01)	2.177e+00 (2.166e+00,2.188e+00)	n5k2id22979 (8.630e-02)
32768	6.789e-01 (6.766e-01,6.810e-01)	2.176e+00 (2.169e+00,2.184e+00)	n5k2id22979 (8.632e-02)
65536	6.784e-01 (6.769e-01,6.799e-01)	2.178e+00 (2.173e+00,2.184e+00)	n5k2id22979 (8.560e-02)
131072	6.788e-01 (6.777e-01,6.798e-01)	2.181e+00 (2.177e+00,2.185e+00)	n5k2id22979 (8.539e-02)

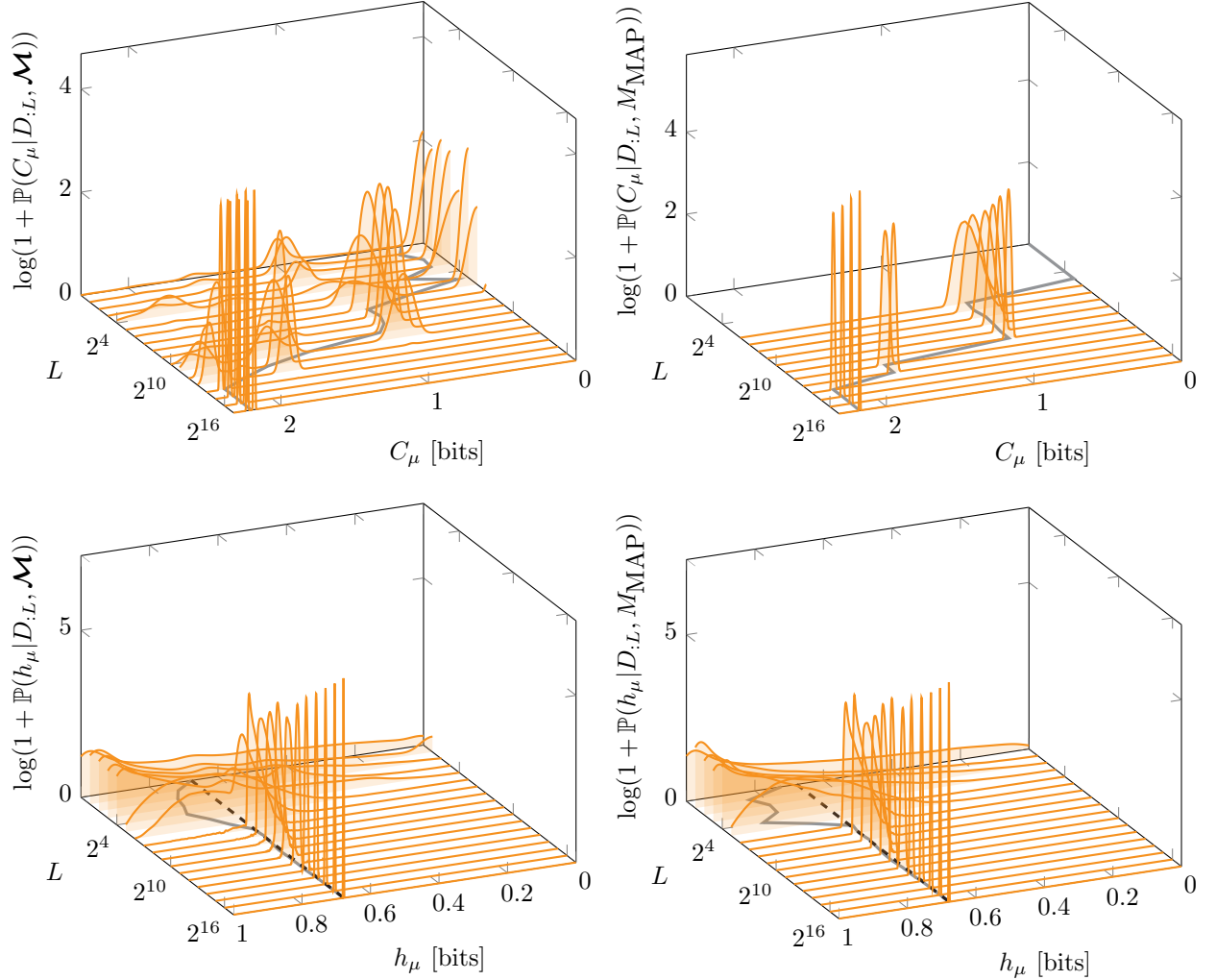


FIG. S7. Simple Nonunifilar Source, $\beta = 4$: Convergence of the posterior densities for C_μ (top) and h_μ (bottom) as a function of subsample length L using the set of all topological ϵ -machines with one- to five-states \mathcal{M} (left column) and the maximum a posteriori model M_{MAP} (right column). In each panel, the black, dashed line indicates the true value and the gray, solid line shows the posterior mean.

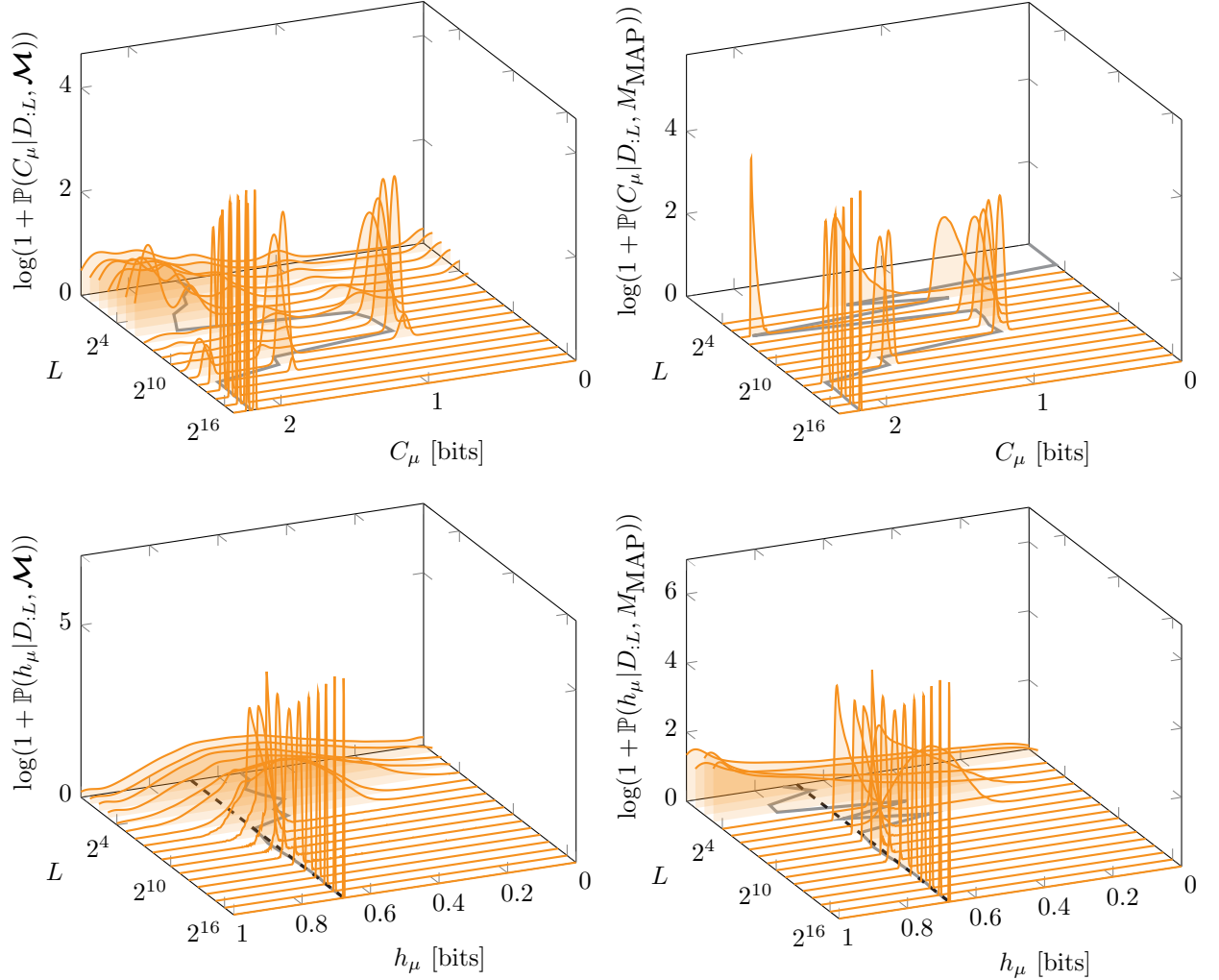


FIG. S8. Simple Nonunifilar Source, $\beta = 2$: Convergence of the posterior densities for C_μ (top) and h_μ (bottom) as a function of subsample length L using the set of all topological ϵ -machines with one- to five-states \mathcal{M} (left column) and the maximum a posteriori model M_{MAP} (right column). In each panel, the black, dashed line indicates the true value and the gray, solid line shows the posterior mean.

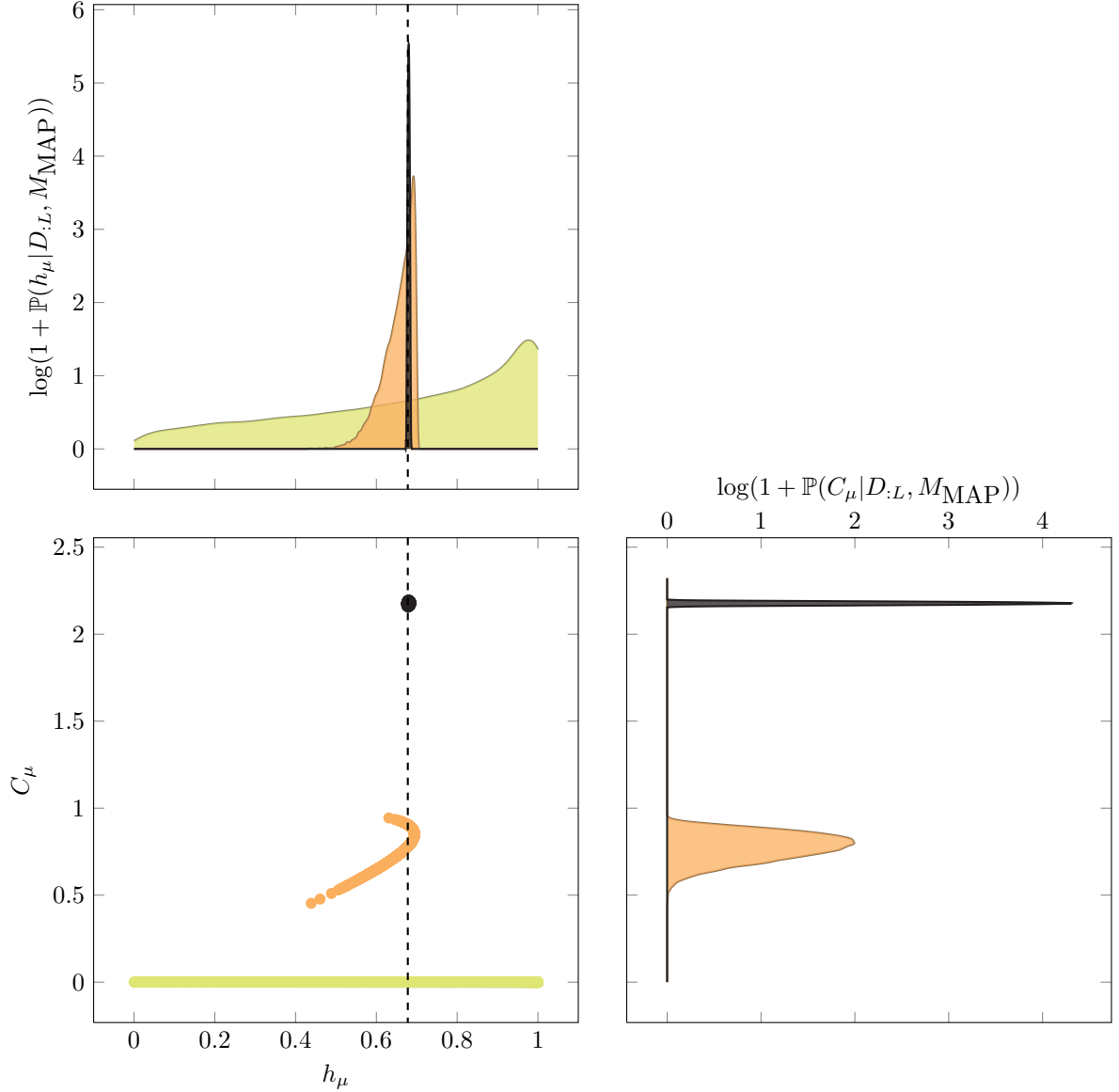


FIG. S9. Simple Nonunifilar Source, $\beta = 4$: Joint distribution samples using the MAP model at the given lengths instead of the full set of candidate models. Colors correspond to data subsample length, as in previous plots. The MAP topology for $L = 1$ (light/beige) has one state and $C_\mu = 0$, as indicated by the samples in the $h_\mu - C_\mu$ plane. No Gkde approximation of these samples is provided due to this complete lack of variation.

V. NUMBER OF ACCEPTING TOPOLOGIES FOR PROCESSES

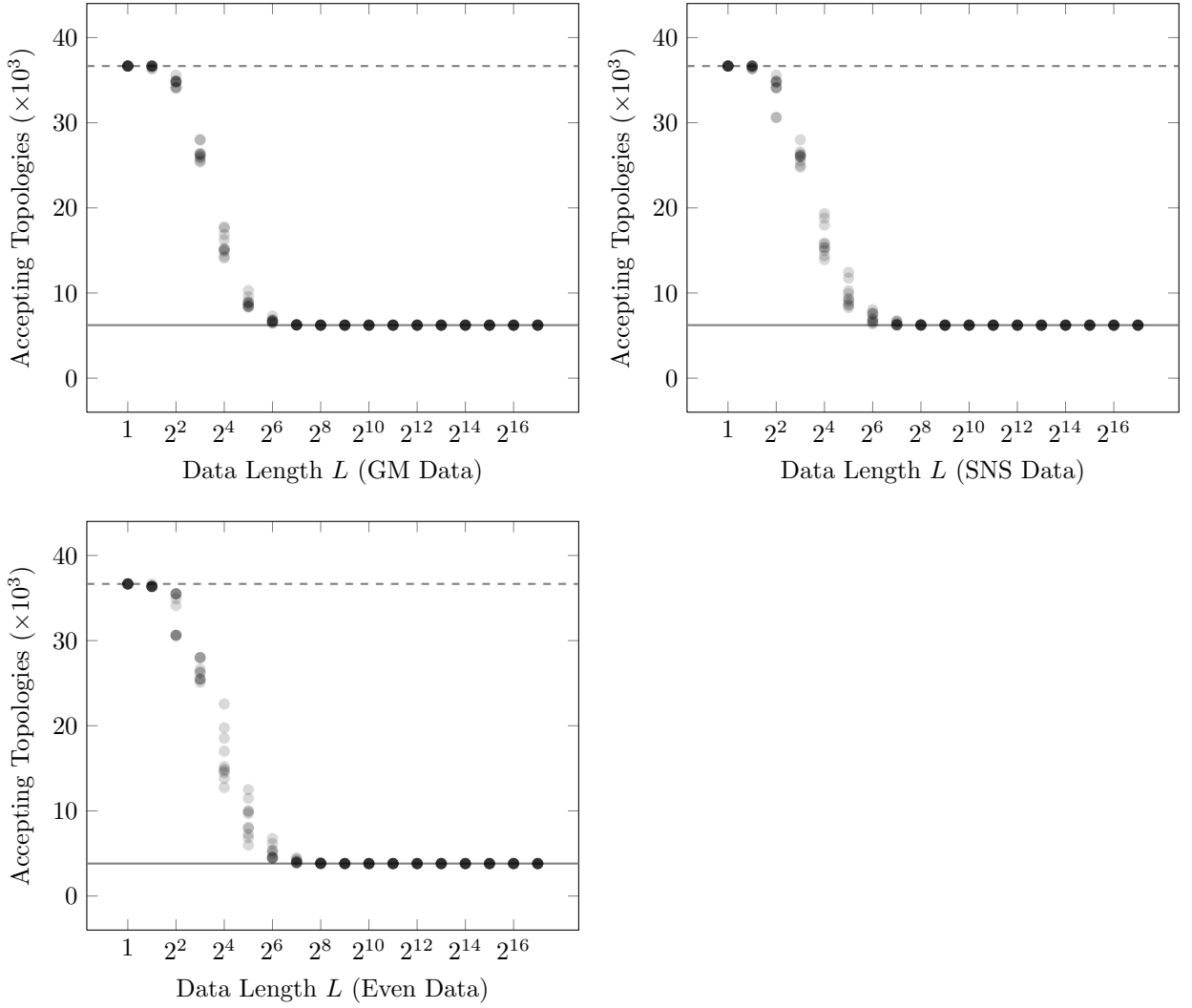


FIG. S10. Number of accepting topologies for each of example processes as a function of subsample length L . For each, a set of ten data series was created and subsamples of length L were analyzed to determine the number of binary-alphabet, one- to five-state topological ϵ -machines that had at least one valid path for that length. (This would result in nonzero likelihood and posterior probability.) For each data series, a gray point is plotted. Overlapping gray points, created by multiple data series with the same number of accepting topologies at the given value of L generate a darker gray or black point. The horizontal lines indicate the total number of candidate structures (36,660, gray dashed line) and the asymptotic number of accepting topologies (solid, gray line). For the Even Process (bottom, left panel), 3,813 topologies were asymptotically accepting whereas the Golden Mean Process (top, left panel) and Simple Nonunifilar Source (top, right panel) both had 6,225.

VI. MAXIMUM A POSTERIORI TOPOLOGIES

Figure S11 lists all MAP topologies encountered when inferring ϵ -machine structure using data from the Even, Golden Mean, and SNS Processes. All processes had n1k2id3 (panel A) as the MAP topology for small L , reflecting a preference for small structures when limited data is available. The Golden Mean Process transitioned from n1k2id3 to n2k2id5 (panel B), the correct structure, at $L = 64$, as documented in Table S2. In a similar manner, the Even Processes changed from n1k2id3 to n2k2id7 (panel C), the correct structure, at data size $L = 32$, as shown in Table S4. The fact that these in-class ϵ -machine structures quickly converge on the correct topology is perhaps expected. Predicting the sample size at which this occurs, however, is not obvious.

The Simple Nonunifilar Source has a more complicated series of MAP topologies, starting with the simple n1k2id3 and progressing through n2k2id5 (panel B), to n4k2id3334 (panel D) and, finally, to n5k2id22979 (panel E) at data size 2^{17} . Of course, this out-of-class data source cannot be exactly captured by the set of finite-state unifilar ϵ -machines considered here. Nonetheless, we expect the size of the inferred model to increase if more data from the SNS were employed and a larger numbers of states were allowed. It is important to note that the MAP structure in this case has very low posterior probability. As discussed in the main text, the topology listed is one of five similar structures with nearly equal posterior probabilities.

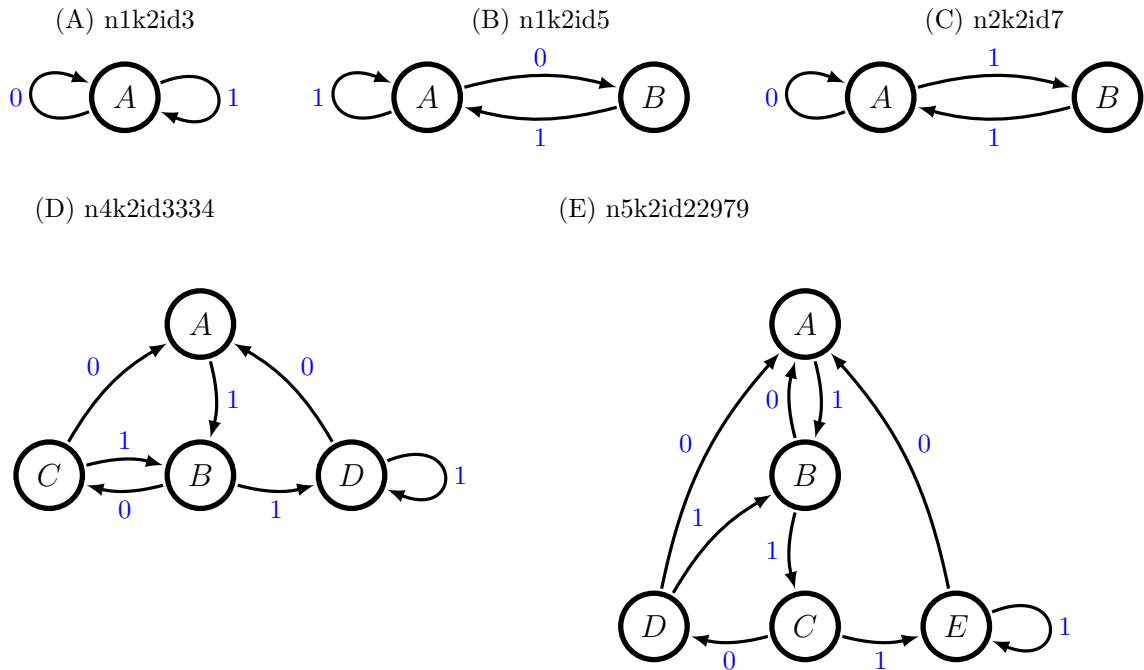


FIG. S11. *Maximum a posteriori* topologies for the Golden Mean, Even, and SNS Process data series. Transitions are only listed with emitted output symbol. Transition probabilities are inferred from data for states that have more than one out-going transition. Transitions from states with only one out-going arc must have probability one, by definition of the topology. Consult Tables S2, S4, and S6 to see when these structures corresponded to the MAP topologies for the given data sources.